Structural and Electron Self-Exchange Rate Variations in Isomeric (Hexaamine)cobalt(III/II) Complexes

Paul V. Bernhardt,* Lathe A. Jones, and Philip C. Sharpe

Department of Chemistry, University of Queensland, Brisbane 4072, Australia

Received November 6, 1996[⊗]

The syntheses and characterisation of the new macrocyclic hexaamine *trans*-(5(*S*),7(*S*),12(*R*),14(*R*)-tetramethyl)-1,4,8,11-tetraazacyclotetradecane-6,13-diamine (L^6) and its Co^{III} complex are reported. The X-ray crystal structural analyses of $[CoL^6]Cl_2(ClO_4)$ [monoclinic, space group $C2/c$, $a = 16.468(3)$ Å, $b = 9.7156(7)$ Å, $c = 15.070(3)$ Å, $\beta = 119.431(8)°$, $Z = 4$] and the closely related *cis*-diamino-substituted macrocyclic complex $[CoL^2](ClO_4)_3 \cdot 2H_2O$ (L^2 = *cis*-6,13-dimethyl-1,4,8,11-tetraazacyclotetradecane-6,13-diamine) [orthorhombic, space group $Pna2_1$, $a = 16.8220(8)$ Å, $b = 10.416(2)$ Å, $c = 14.219(3)$ Å, $Z = 4$] reveal significant variations in the observed Co−N bond lengths and coordination geometries, which may be attributed to the *trans* or *cis* disposition of the pendent primary amines. The $Co^{III/II}$ self-exchange electron transfer rate constants for these and other closely related hexaamines have been determined, and variations of some 2 orders of magnitude are found between pairs of *trans* and *cis* isomeric Co^{III} complexes.

Introduction

(Hexaamine)cobalt(III) complexes, by virtue of their abundance and diversity, have played a fundamental role in our understanding of the structural, spectroscopic and electrochemical properties of coordination compounds.[1] There exists a vast array of Co^{III} complexes bearing six saturated N-donors, ranging from the simplest case $[Co(NH_3)_6]^{3+}$ through to macrocyclic hexaamine ligands. The variety of physical properties exhibited by (hexaamine)cobalt(III) complexes is illustrated by (i) structural studies revealing Co−N bond lengths ranging from 1.93 to 2.04 Å; (ii) electrochemical measurements identifying $Co^{III/II}$ redox couples spanning almost 1 V, and (iii) spectroscopy which has found visible electronic maxima varying between 520 and 440 nm. Electron transfer reactions of Co^{III} hexaamines have received special attention,[2,3] and a number of studies have now demonstrated their overall compliance with Marcus theory.[4] Of particular interest has been the remarkable variation in $Co^{III/II}$ hexaamine self-exchange electron transfer rates across some 9 orders of magnitude. This variation has been the subject of considerable experimental and theoretical attention.[5]

In earlier reports,[6,7] we have investigated the syntheses, spectroscopy, and structures of a number of complexes of the isomeric macrocyclic hexaamines L^1 and L^2 (see Chart 1). These ligands are derived from metal-directed cyclization reactions of $[Cu(en)_2]^{2+}$ (en = ethane-1,2-diamine) with nitroethane and formaldehyde, followed by reduction to afford the metal-free hexaamines. The Co^{III} complex of L^1 exhibits some quite remarkable properties,[8] namely (i) short Co−N bond lengths, (ii) a particularly negative $Co^{III/II}$ redox couple, and (iii) a $Co^{III/II}$ self-exchange electron transfer rate constant more than 2 orders of magnitude greater than any other (hexaamine)cobalt(III/II) system. It is not intuitively obvious that these three properties should be related, and we have been interested in studying other structural analogues of $[CoL^1]^{3+}$ in order to explain these unusual observations. The metal-directed chemistry ultimately leading to L^1 and its complexes may be extended to ligands with different alkyl chains attached to the ring (L^3 and L^4),[9] while retaining the same diamino-substituted 14-membered macrocyclic structural unit. Recently, we reported[10] a variation on this chemistry by using a combination of acetaldehyde and nitromethane as the cyclization reagents, resulting in the dinitro−tetramethyl-substituted macrocyclic ligand L^5 as its Cu^{II} complex. In this work, we report the synthesis of the new hexaamine L^6 from reduction of the complex $[CuL^5]^{2+}$, and also the hexadentate-coordinated Co^{III} complex of L^6 has been produced. In addition we have undertaken a study of the self-exchange electron transfer properties of this complex $[CoL^6]^{3+}$ and the pairs of isomeric hexaamines $[CoL^1]^{3+}/[CoL^2]^{3+}$ and $[CoL^3]^{3+}/[CoL^4]^{3+}$. We will demonstrate that some significant

Chart 1

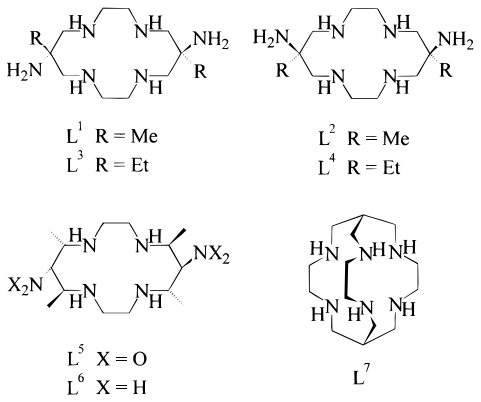

[⊗] Abstract published in *Advance ACS Abstracts,* May 1, 1997.

(1) Hendry, P.; Ludi, A. *Adv. Inorg. Chem.* **1990**, *35*, 117.
(2) Creaser, I. I.; Sargeson, A. M.; Zanella, A. W. *Inorg. Chem.* **1983**, *22*, 4022.
(3) Endicott, J. F.; Brubaker, G. R.; Ramasami, T.; Kumar, K.; Dwarakanath, K.; Cassel, J.; Johnson, D. *Inorg. Chem.* **1983**, *22*, 3754.
(4) Marcus, R. A. *Angew. Chem., Int. Ed. Engl.* **1993**, *32*, 1111 and references therein.
(5) Meyer, T.; Taube, H. In *Comprehensive Coordination Chemistry*; Wilkinson, G., Ed.; Pergamon: London, **1987**.
(6) Bernhardt, P. V.; Comba, P.; Hambley, T. W.; Lawrance, G. A. *Inorg. Chem.* **1991**, *30*, 942 and references therein.
(7) Bernhardt, P. V.; Comba, P.; Hambley, T. W. *Inorg. Chem.* **1993**, *32*, 2804 and references therein.
(8) Bernhardt, P. V.; Lawrance, G. A.; Hambley, T. W. *J. Chem. Soc., Dalton Trans.* **1989**, 1059.
(9) Bernhardt, P. V.; Byriel, K. A.; Kennard, C. H. L.; Sharpe, P. C. *Inorg. Chem.* **1996**, *35*, 2045.
(10) Bernhardt, P. V.; Byriel, K. A.; Kennard, C. H. L.; Sharpe, P. C. *J. Chem. Soc., Dalton Trans.* **1996**, 145.

S0020-1669(96)01345-6 CCC: $14.00

differences in the electron transfer properties of these closely related systems arise as a result of subtle structural variations across the series.

Experimental Section

Safety Note. *Caution: Perchlorate salts are potentially explosive!* Although we have experienced no problems with the compounds reported in this work, they should only be handled in small quantities and never scraped from sintered glass frits nor heated in the solid state.

Syntheses. The complexes $Na_3[Co(CO_3)_3]$,[11] (*trans*-6,13-dimethyl-1,4,8,11-tetraazacyclotetradecane-6,13-diamine)cobalt(III) perchlorate ($[CoL^1](ClO_4)_3$),[8] (*cis*-6,13-dimethyl-1,4,8,11-tetraazacyclotetradecane-6,13-diamine)cobalt(III) perchlorate ($[CoL^2](ClO_4)_3$),[7] (*trans*-6,13-diethyl-1,4,8,11-tetraazacyclotetradecane-6,13-diamine)cobalt(III) perchlorate ($[CoL^3](ClO_4)_3$),[9] (*cis*-6,13-diethyl-1,4,8,11-tetraazacyclotetradecane-6,13-diamine)cobalt(III) perchlorate ($[CoL^4](ClO_4)_3$),[9] and (*trans*-6,13-dinitro-(5(*S*),7(*S*),12(*R*),14(*R*)-tetramethyl)-1,4,8,11-tetraazacyclotetradecane)copper(II) perchlorate ($[CuL^5](ClO_4)_2$)[10] were prepared from literature syntheses.

Crystals of $[CoL^2](ClO_4)_3 \cdot 2H_2O$ suitable for X-ray work were grown by slow evaporation of an aqueous solution of the complex and excess $NaClO_4$.

***trans*-(5(*S*),7(*S*),12(*R*),14(*R*)-Tetramethyl)-1,4,8,11-tetraazacyclotetradecane-6,13-diamine Hexahydrochloride, $L^6 \cdot 6HCl$.** A solution of $[CuL^5](ClO_4)_2$ (14.6 g) in water (1.5 L) was acidified with HCl (150 mL, 32%). This solution was added slowly in portions to excess Zn dust (20 g) with vigorous stirring, such that no residual purple color remained when the next aliquot was added. The colorless mixture was then gravity filtered to remove solids and applied to a 1 m × 2 cm column of Dowex 50WX2 cation-exchange resin (H^+ form). The column was washed with 1 M HCl to remove Zn_{aq}^{2+} (identified by neutralizing aliquots of the eluate to afford a precipitate of $Zn(OH)_2$). The protonated ligand eluted slowly with 3 M HCl (higher acid concentrations resulted in precipitation of the hydrochloride salt of the ligand on the column). The eluent was concentrated to *ca.* 100 mL on a rotary evaporator to afford a colorless precipitate, which was collected by filtration, washed with ethanol and then diethyl ether, and dried in a vacuum desiccator (8.3 g, 68%). The filtrate was evaporated to dryness to afford an oil whose ^1H and ^{13}C NMR spectra were identical to that of the isolated precipitate. Anal. Calcd for $C_{14}H_{40}Cl_6N_6 \cdot 4H_2O$: C, 29.1; H, 8.4; N, 14.6. Found: C, 29.1; H, 8.4; N 14.4. ^1H NMR (D_2O): δ 1.36 (doub., CH_3), 1.38 (doub., CH_3), 2.9−3.2 (mult., CH_2/CH), 3.4 (doub. of doub., CH), ∼3.6 (2 × singl. CH_2), 3.70 (quart., CH). ^{13}C NMR (D_2O): δ 13.2, 16.4 (CH_3), 46.0, 46.3(CH_2), 54.1, 55.8, 56.8 (CH).

***trans*-(5(*S*),7(*S*),12(*R*),14(*R*)-Tetramethyl)-1,4,8,11-tetraazacyclotetradecane-6,13-diaminecobalt(III) Perchlorate.** A solution of $Na_3[Co(CO_3)_3]$ (0.77 g) and $L^6 \cdot 6HCl \cdot 4H_2O$ (1.04 g) in water (100 mL) was stirred at 80 °C for 1 h. The resulting yellow solution was diluted to *ca.* 2 L and applied to a 500 × 3 cm column of Sephadex C-25 cation-exchange resin (Na^+ form). The complex eluted as the only band of significant intensity with 3 M $NaClO_4$ solution. Upon concentration to *ca.* 50 mL the complex precipitated as a yellow powder. This was collected by filtration (*see Safety Note*) and washed with ethanol and diethyl ether (0.20 g). Further crops were obtained from the filtrate. Anal. Calcd for $C_{14}H_{34}Cl_3CoN_6O_{12}$: C,26.1; H, 5.3; N, 13.1. Found: C, 26.0; H, 5.4; N 13.0. ^1H NMR (D_2O): δ 1.42 (doub., CH_3), 1.43 (doub., CH_3), 3.0−3.4 (mult., CH_2/CH), 3.86 (quart., CH). ^{13}C NMR (D_2O): δ 12.0, 13.7 (CH_3), 46.9 (CH_2), 53.3, 54.0, 61.2 ppm (CH). Crystals of the mixed salt $[CoL^6]Cl_2(ClO_4)$ suitable for X-ray work were grown from the filtrate above after acidification with HCl.

Physical Methods. ^1H and proton-decoupled ^{13}C nuclear magnetic resonance spectra were measured at 200 and 50.32 MHz, respectively, on a Bruker AC200 spectrometer, with chemical shifts cited *vs* tetramethylsilane. Solution UV−vis spectra were measured on a Perkin-Elmer Lambda 12 spectrophotometer. Cyclic voltammetry was performed with a BAS 100B electrochemical analyzer employing a glassy carbon working electrode, an Ag/AgCl reference electrode, and a Pt auxiliary electrode. DC polarography was performed with a Metrohm E 506 potentiostat with a Model E 505 dropping Hg electrode, a saturated calomel reference electrode, and a Pt auxiliary electrode. All solutions for electrochemistry were *ca.* 5×10^{-3} M in analyte and 0.1 M in $NaClO_4$ and were purged with N_2 before measurement.

Pulse radiolysis experiments were performed with a van de Graaff electron accelerator which delivered electron pulses (3 μs) at *ca.* 1 MeV through the thin wall of a cell with a 1 cm optical path as previously described.[12] Dosimetry was performed with an N_2O-saturated solution of KSCN by employing a value of $\epsilon_{480\ nm}[(SCN)_2^{\bullet-}] = 7600\ M^{-1}\ cm^{-1}$. Radiolytically initiated electron transfer reactions were performed on solutions containing 0.02 M $ZnSO_4$ (pH 6.0, 298 K) and *ca.* 0.01 M *tert*-BuOH as an OH radical scavenger. Decay of Zn_{aq}^+ (the product of the reaction between Zn_{aq}^{2+} and e_{aq}^-) under pseudo-first-order conditions was monitored at 310 nm for Co^{III} concentrations of 0, 1, 2, 3, 4, and 5×10^{-4} M. Plots of k_{obs} *vs* [Co^{III}] appear in the Supporting Information.

Calculations. Molecular mechanics trial structures were built with the program HyperChem and minimized with MOMECPC[13] using a published force field,[14] except for the Co^{II}−N parameters (k and r_0) which have been reported elsewhere.[15] Importantly, the remaining parameters in this force field[14] (C−C, C−N, C−C−C, *etc.*) are the same as those found in the force field from which the Co^{II}−N constants were taken.[15]

X-ray Crystal Structure Analyses. Cell constants were determined by a least-squares fit to the setting parameters of 25 independent reflections measured on an Enraf-Nonius CAD4 four-circle diffractometer employing graphite-monochromated Mo Kα radiation and operating in the $\omega-2\theta$ scan mode. Data reduction and empirical absorption corrections (ψ-scans) were applied with the XTAL package.[16]

Both structures were solved by heavy atom methods with SHELXS-86[17] and refined by full-matrix least-squares analysis with SHELXL-93.[18] All non-H atoms were refined with anisotropic thermal parameters, whereas H atoms were included at estimated positions. Crystal data are assembled in Table 1, and the atomic nomenclature is defined in Figures 1 and 2 drawn with the program PLATON.[19] Selected bond lengths and angles are assembled in Table 2.

Table 1. Crystal Data

	$[CoL^6]Cl_2(ClO_4)$	$[CoL^2](ClO_4)_3 \cdot 2H_2O$
space group	*C*2/*c* (No. 15)	*Pna*2$_1$ (No. 33)
formula	$C_{14}H_{34}Cl_3CoN_6O_4$	$C_{12}H_{34}Cl_3CoN_6O_{14}$
a, Å	16.468(3)	16.8220(8)
b, Å	9.7156(7)	10.416(2)
c, Å	15.070(3)	14.219(3)
β, deg	119.431(9)	
V, Å^3	2100.0(6)	2491.4(7)
ρ_{calcd}, g cm^{-3}	1.631	1.738
fw	515.75	651.73
Z	4	4
μ, cm^{-1}	12.33	10.88
temp, °C	23	23
λ, Å	0.710 73	0.710 73
N	1850	2277
N_o ($F_o > 2\sigma$)	1591	2127
$2\theta_{max}$, deg	50	50
$R(F_o)$,[a] $wR_2(F_o^2)$[b]	0.030, 0.077[c]	0.031, 0.084[d]

[a] $R(F_o) = \sum||F_o| - |F_c||\sum|F_o|$. [b] $wR_2(F_o^2) = (\sum w(F_o^2 - F_c^2)^2 / \sum wF_o^2)^{1/2}$. [c] $w = (\sigma^2(F_o^2) + (0.0497P)^2 + 2.07P)^{-1}$. [d] $w = (\sigma^2(F_o^2) + (0.0632P)^2 + 1.03P)^{-1}$, where $P = {}^1/_3[\max(F_o^2,0)] + {}^2/_3F_c^2$.

(11) Bauer, H. F.; Drinkard, W. C. *Inorg. Synth.* **1966**, *8*, 202.

(12) Boucher, H. A.; Sargeson, A. M.; Sangster, D. F.; Sullivan, J. C. *Inorg. Chem.* **1981**, *20*, 3719.

(13) Comba, P.; Hambley, T. W. MOMECPC: A Molecular Mechanics Program for Coordination Compounds, Universities of Heidelberg and Sydney.

(14) Bernhardt, P. V.; Comba, P. *Inorg. Chem.* **1992**, *31*, 2638.

(15) Bond, A. M.; Hambley, T. W.; Snow, M. R. *Inorg. Chem.* **1985**, *24*, 1920.

(16) Hall, S. R., Flack, H. D., Stewart, J. M., Eds., The XTAL3.2 User's Manual, Universities of Western Australia, Geneva, and Maryland.

(17) Sheldrick, G. M. *Acta Crystallogr.* **1990**, *A46*, 467.

(18) Sheldrick, G. M. SHELXL93: Program for Crystal Structure Determination, University of Göttingen, 1993.

(19) Spek, A. L. *Acta Crystallogr.* **1990**, *A46*, C34.

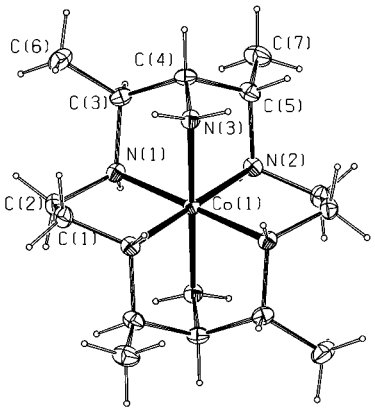

Figure 1. View of the $[CoL^6]^{3+}$ ion showing 30% thermal ellipsoids.

Results

The new macrocyclic ligand L^6 (Chart 1) was obtained in good yield from a Zn/HCl reduction of the dinitro precursor complex $[CuL^5]^{2+}$. NMR spectroscopy showed that the reduction affords but one isomeric form of the ligand, although many isomers are possible based on the absolute configurations of the methyl- and amino-substituted macrocyclic C atoms. Seven distinct resonances were found in the DEPT ^{13}C NMR spectrum of L^6 in acidic solution, indicative of the C_i symmetry of the ligand. The sets of methyl, *C*-methylated, and methylene C atoms each split into magnetically distinct pairs of resonances as a result of the "axial" and "equatorial" dispositions of the methyl groups, while the remaining pair of amino-substituted C atoms are equivalent. The ^1H NMR spectrum of the ligand was complicated by a number of overlapping sets of resonances, and little useful information could be obtained. Complexation of L^6 with Co^{III} was straightforward and led exclusively to the hexadentate-coordinated complex under the reaction conditions employed. By comparison, pentadentate- and tetradentate-coordinated Co^{III} complexes of L^1 have been isolated[8] under slightly different reaction conditions. We have not pursued tetraamine and pentaamine complexes of L^6, although they should be readily accessible.

The X-ray crystal structure analysis of $[CoL^6]Cl_2(ClO_4)$ found the complex cation on a center of symmetry, the perchlorate anion on a 2-fold axis, and the chloride ions on general sites. A view of the cation is given in Figure 1, showing hexadentate coordination of the ligand. The Co−N bond lengths are the same within experimental error (Table 2) and are shorter than those usually found in a typical (hexaamine)cobalt(III) ion (Table 3). There is a significant angular distortion of the CoN_6 octahedron. This is most apparent upon inspection of the N(1,2)−Co−N(3) angles within the two fused five-membered chelate rings, which are both contracted by ∼5° from those of an ideal octahedron. An eclipsed conformation of the two ethylenediamine residues (*trans-eq,eq*)[20] is defined. No conformational disorder of this five-membered chelate ring is evident upon inspection of the C atom thermal ellipsoids and C−C or C−N bond lengths, whereas disorder of this kind has been found in a number of structures of hexadentate-coordinated complexes of L^1 and L^3.[6,9,21,22]

The ^{13}C NMR spectrum of $[CoL^6]^{3+}$ was qualitatively similar to that of the metal-free ligand, except that the anticipated pair of methylene resonances derived from the ethane-1,2-diamine residues were accidentally degenerate in the spectrum. The ^1H NMR spectrum of $[CoL^6]^{3+}$ was rather complicated on the whole. However, a quite prominent quartet was observed at ∼3.8 ppm, well separated from the remaining cluster of methylene and methine proton resonances (3.0−3.4 ppm). The quartet may be assigned to an H atom *gem* to one of the methyl groups. Inspection of the two H−C−C−H dihedral angles (ϕ) in the six-membered chelate ring (Figure 1) indicates that coupling between the proton attached to C(4) and the two vicinal methine protons will be quite different *i.e.* ϕ(H−C(5)−C(4)−H) 56°, $^3J \sim 2-3$ Hz, and ϕ(H−C(3)−C(4)−H) 84°, $^3J \sim 0$ Hz. Therefore, the proton attached to C(3) corresponds to the observed quartet, whereas the anticipated quartet of doublets due to the H atom attached to C(5) is buried among the remaining methylene and methine resonances.

Table 2. Selected Bond Lengths (Å) and Angles (deg) for $[CoL^6]^{3+}$ and $[CoL^2]^{3+}$

	$[CoL^6]^{3+}$	$[CoL^2]^{3+}$
Co(1)−N(1)	1.949(2)	1.962(4)
Co(1)−N(2)	1.943(2)	1.959(4)
Co(1)−N(3)	1.942(2)	1.936(4)
Co(1)−N(4)		1.964(3)
Co(1)−N(5)		1.960(3)
Co(1)−N(6)		1.960(4)
N(3)−Co(1)−N(2)	85.78(8)	87.5(2)
N(3)−Co(1)−N(1)	84.11(8)	178.8(2)
N(2)−Co(1)−N(1)	90.91(8)	92.1(2)
N(3)−Co(1)−N(5)		98.3(2)
N(2)−Co(1)−N(5)		83.5(2)
N(3)−Co(1)−N(6)		83.1(2)
N(2)−Co(1)−N(6)		170.5(2)
N(5)−Co(1)−N(6)		99.0(2)
N(5)−Co(1)−N(1)		82.7(2)
N(6)−Co(1)−N(1)		97.3(2)
N(3)−Co(1)−N(4)		92.6(2)
N(2)−Co(1)−N(4)		96.0(2)
N(5)−Co(1)−N(4)		169.0(2)
N(6)−Co(1)−N(4)		83.3(2)
N(1)−Co(1)−N(4)		86.3(2)

The aqueous solution UV−vis electronic spectrum of $[CoL^6]^{3+}$ exhibited two spin−allowed d−d transitions characteristic of a low-spin d^6 ion in a pseudooctahedral ligand field. The transitions (λ_{max} 441 nm (ϵ 71.6 M^{-1} cm^{-1}, $^1T_{1g} \leftarrow {}^1A_{1g}$) and 325 nm ($\epsilon$ 63.1, $^1T_{2g} \leftarrow {}^1A_{1g}$)) occur at higher energy than any other (hexaamine)cobalt(III) complex (Table 3). The relatively small extinction coefficients are indicative of a centrosymmetric ligand field.

Cyclic voltammetry of $[CoL^6]^{3+}$ on a glassy carbon working electrode identified a totally reversible $Co^{III/II}$ couple at −0.55 V *vs* NHE. There was no variation in the anodic/cathodic current ratio (i_a/i_c) as a function of scan rate indicating that the reduced complex is stable on the voltammetric time scale. A slight increase in cathodic and anodic peak separation (ΔE_p) was found with increasing scan rate. The redox potential of the complex is at the more negative end of the range of known (hexaamine)cobalt(III/II) couples (Table 3).

The X-ray crystal structure of $[CoL^2](ClO_4)_3 \cdot 2H_2O$ is isostructural with its Cr^{III} analogue, with all molecules situated at general positions. The folded conformation of the macrocycle is apparent in Figure 2, with the two primary amines coordinating in *cis* coordination sites as dictated by the geometry of the hexadentate ligand. The Co−N bond lengths (average 1.96 Å) are significantly longer than those found in the corresponding *trans* isomer $[CoL^1]^{3+}$ (average 1.94 Å). The same trend in M−N bond lengths going from $[ML^1]^{n+}$ to $[ML^2]^{n+}$ has now

(20) The nomenclature refers to the equatorial or axial orientation of the H atoms attached to C(1)/C(2) *trans* to the adjacent secondary amine H atom.

(21) Bernhardt, P. V.; Comba, P.; Curtis, N. F.; Hambley, T. W.; Lawrance, G. A.; Maeder, M.; Siriwardena, A. *Inorg. Chem.* **1990**, *29*, 3208.

(22) Bernhardt, P. V.; Lawrance, G. A.; Hambley, T. W. *J. Chem. Soc., Dalton Trans.* **1990**, 983.

Table 3. Physical Data for (Hexaamine)cobalt(III) Complexes (Data in Parentheses Predicted by Molecular Mechanics)

	$Co^{III}-N_{av}$ (Å)	$Co^{II}-N_{av}$ (Å)	λ_{max} (nm)	$E°$ (V vs SHE)	k_{12} (M^{-1} s^{-1})	k_{11} (M^{-1} s^{-1})	ΔU_{tot} (kJ mol^{-1})
$[Co(NH_3)_6]^{3+}$	1.96[a]	2.17[b]	472, 338[c]	−0.04[d]	8.4×10^8 [e]	$\sim 10^{-6}$ [f]	54
$[Co(en)_3]^{3+}$	1.96[g]	(2.16)	464, 338[c]	−0.20[d]	2.5×10^8 [e]	3.4×10^{-5} [h]	52
$[CoL^1]^{3+}$	1.94[i]	(2.10)	447, 328[i]	−0.57[i]	1.3×10^8	680	41
$[CoL^2]^{3+}$	1.96	(2.14)	459, 334[j]	−0.44[j]	1.6×10^8	6.6	47
$[CoL^3]^{3+}$	1.95[k]	(2.10)	450, 330[k]	−0.58[k]	1.1×10^8	720	41
$[CoL^4]^{3+}$	(1.96)	(2.14)	460, 336[k]	−0.48[k]	4.4×10^7	2.3	47
$[CoL^6]^{3+}$	1.94	(2.12)	441, 325	−0.55	1.7×10^8	540	42
$[CoL^7]^{3+}$	1.97[i]	2.17[m]	471, 343[n]	−0.43[d]	1.1×10^8 [o]	2.1[p]	40

[a] Figgis, B. N.; Skelton, B. W.; White, A. H. *Aust. J. Chem.* **1979**, *32*, 417. [b] Unpublished work cited in: Hambley, T. W. *Inorg. Chem.* **1988**, *27*, 2496. [c] Jørgensen, C. K. *Adv. Chem. Phys.* **1963**, *5*, 33. [d] Bond, A. M.; Lawrance, G. A.; Lay, P. A.; Sargeson, A. M. *Inorg. Chem.* **1983**, *22*, 2010. [e] Meyerstein, D.; Mulac, W. A. *J. Phys. Chem.* **1969**, *73*, 1091. [f] Hammershøi, A.; Geselowitz, A.; Taube, H. *Inorg. Chem.* **1984**, *23*, 979. [g] Average of 27 structures from the Cambridge Data Base. [h] Dwyer, F. P; Sargeson, A. M. *J. Phys. Chem.* **1961**, *65*, 1892. [i] Reference 8. [j] Reference 7. [k] Reference 9. [l] Clark, I. J.; Geue, R. J.; Engelhardt, L. M.; Harrowfield, J. M.; Sargeson, A. M.; White, A. H. *Aust. J. Chem.* **1993**, *46*, 1485 (dihydroxy-substituted analogue). [m] Unpublished work cited in: Comba, P. *Inorg. Chem.* **1989**, *28*, 426 (diammonio-substituted analogue). [n] Hambley, T. W.; Geue, R. J.; Harrowfield, J. M.; Sargeson, A. M.; Snow, M. R. *J. Am. Chem. Soc.* **1984**, *106*, 5478. [o] Unpublished work cited in ref 8. [p] Reference 2.

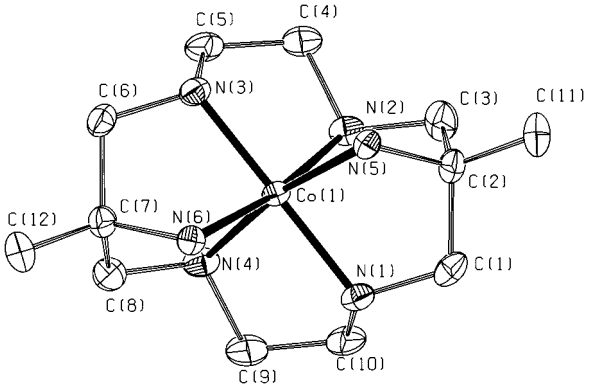

Figure 2. View of the $[CoL^2]^{3+}$ ion showing 30% thermal ellipsoids. H atoms are omitted for clarity.

been observed in the Co^{III}, Cr^{III}, and Ni^{II} complexes,[7,23] which is consistent with earlier molecular mechanics predictions.[24] The spectrocopic and electrochemical properties of this complex have been reported previously.[7]

The electron transfer cross-reaction rate constants (k_{12}) for the reaction between Zn^+ and each of the complexes $[CoL^1]^{3+}$, $[CoL^2]^{3+}$, $[CoL^3]^{3+}$, $[CoL^4]^{3+}$, and $[CoL^6]^{3+}$ (eq 1) were determined under pseudo-first-order conditions.

$$Zn^+ + [CoL^x]^{3+} \xrightarrow{k_{12}} Zn^{2+} + [CoL^x]^{2+} \qquad (1)$$

According to the so-called Marcus cross-relation,[4] the bimolecular rate constant for this reaction is given by eq 2, where

$$k_{12} = (k_{11}k_{22}K_{12}f_{12})^{1/2} \qquad (2)$$

k_{11} and k_{22} are the $[CoL^x]^{3+/2+}$ and $Zn^{2+/+}$ self-exchange rate constants, respectively, and f_{12} is a frequency factor which we have assumed to be unity, as is often the case. The equilibrium constant K_{12} for eq 1 may be determined from the standard redox potentials of the two couples as given in eq 3.

$$K_{12} = \exp\left[\frac{nF}{RT}(E°([CoL^x]^{3+/2+}) - E°(Zn^{2+/+}))\right] \qquad (3)$$

The unknown $Zn^{2+/+}$ self-exchange rate constant (k_{22}) and the poorly defined redox potential ($E°(Zn^{2+/+})$) may be eliminated from eqs 2 and 3 by using data from the related hexaamine $[CoL^7]^{3+/2+}$, whose self-exchange rate (2.1 M^{-1} s^{-1}),[2] redox potential (−0.43 V *vs* SHE),[2] and Zn^I cross-reaction rate constant (1.1×10^8 M^{-1} s^{-1})[8] are known (Table 3). This leads to an expression for the self-exchange rate constant of each complex in terms of its observed cross-reaction rate constant and redox potential (eq 4)

$$k_{11}([CoL^x]^{3+/2+}) = 2.1\left[\frac{k_{12}}{1.1 \times 10^8}\right]^2 \exp[38.94(-0.43 - E°([CoL^x]^{3+/2+}))] \qquad (4)$$

The experimental values of k_{12} are given in Table 3, as well as the calculated self-exchange rate constants k_{11}. The k_{11} values of the pairs of *trans* and *cis* isomers, *i.e.* $[CoL^1]^{3+/2+}$/$[CoL^2]^{3+/2+}$ and $[CoL^3]^{3+/2+}$/$[CoL^4]^{3+/2+}$, differ by 2 orders of magnitude. The remeasured value of k_{11} for $[CoL^1]^{3+/2+}$ in this work is not significantly different from that originally reported.[8] The *trans* diamino-substituted macrocyclic $[CoL^6]^{3+/2+}$ system also exhibits a large k_{11} value, similar to the structural analogues $[CoL^1]^{3+/2+}$ and $[CoL^3]^{3+/2+}$. This feature will be discussed in greater detail below.

Discussion

As reported previously,[10] the initial macrocyclization reaction leading to the dinitro-substituted complex $[CuL^5]^{2+}$ is remarkably stereoselective, and this is maintained upon reduction to the hexaamine metal-free ligand L^6. That is, we have not been able to identify the corresponding *cis* diamino isomer of L^6 as a reaction product at this time. This is notable as *ca.* 4:1 mixtures of *trans*- and *cis*-hexaamines, *i.e.* L^1/L^2 and L^3/L^4, have been found in similar macrocyclization reactions involving nitroethane[25] and nitropropane[9] as the "locking group". Epimerization of the relatively acidic nitro-substituted C atoms in $[CuL^5]^{2+}$ is possible, and perhaps the observed stereoselectivity arises from an equilibration of the *trans* and *cis* isomers of $[CuL^5]^{2+}$ during the macrocyclization reaction, which evidently favors the *trans* form exclusively. Such an equilibration cannot occur in the dinitro precursors of L^1/L^2 and L^3/L^4 where the *C*-methyl and *C*-ethyl substituents prohibit epimerization of the nitro-substituted C atoms and, thus, noninterconvertible, kinetically determined mixtures of *trans* and *cis* isomers result.

The contribution of intraligand strain energy is a dominant factor in the observed structures of coordination compounds, particularly those bearing chelating ligands. Molecular mechanics calculations allow separate contributions to the overall strain energy of complexes in various conformations to be delineated, and also predictions of structures of unknown compounds may

(23) Bernhardt, P. V. Unpublished results.
(24) Bernhardt, P. V.; Comba, P. *Helv. Chim. Acta* **1991**, *74*, 1834.
(25) Bernhardt, P. V.; Comba, P.; Hambley, T. W.; Lawrance, G. A.; Várnagy, K. *J. Chem. Soc., Dalton Trans.* **1992**, 355.

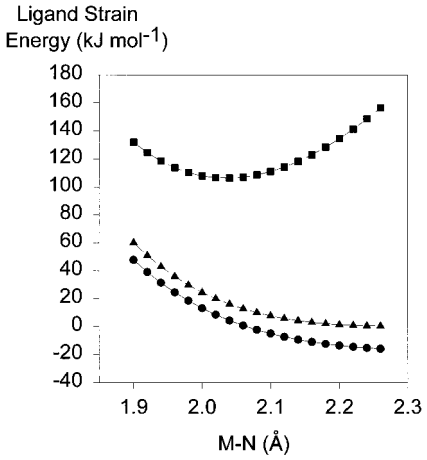

Figure 3. Plots of ligand strain energy (kJ mol^{-1}) as a function of the M−N bond length (Å) for $[M(NH_3)_6]^{n+}$ (●), $[M(en)_3]^{n+}$ (▲, *lel*$_3$ conformation), and $[ML^6]^{n+}$ (■, *trans-eq,eq* conformation).

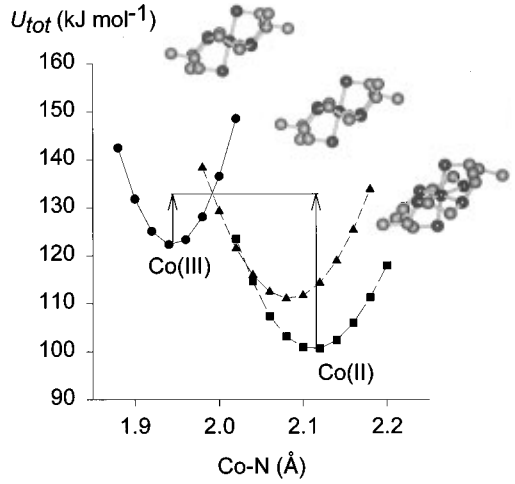

Figure 4. Plots of total strain energy (kJ mol^{-1}) as a function of Co−N bond length (Å) for $[CoL^6]^{3+}$ (●, *trans-eq,eq*), and $[CoL^6]^{2+}$ (▲, *trans-eq,eq*), and $[CoL^6]^{2+}$ (■, *trans-ax,eq*). Arrows indicate contributions from each component of redox couple to the overall changes in molecular mechanics strain energy upon activation (ΔU_{tot}; see Table 3).

be made. In Figure 3, we have plotted the *ligand* strain energy *only* as a function of the M−N bond length for three hexaamine systems. In this case, terms involving the metal ion make no contribution to the strain energy; thus, the plots are generic. For the simple $[M(NH_3)_6]^{n+}$ and $[M(en)_3]^{n+}$ systems, the strain energy continues to decrease with increasing M−N bond length as interligand (N···N) repulsion decreases. Therefore, at least in terms of ligand strain energies, there is no preferred metal ion size for hexaammine or tris(ethane-1,2-diamine) complexes, and the M−N bond length may increase without hindrance by the ligands. The M−N bond lengths in complexes of this type will be dictated by the metal ion (*i.e.* M−N force constant and strain-free bond length) but influenced very little by the ligand. By contrast the geometric constraints inherent to hexadentate-coordinated ligands (*e.g.* L^{1-4}, $L^{6,7}$) typically result in a certain preferred cavity size. If a metal ion is either smaller or larger than the preferred cavity size of the ligand with which it is coordinated, the ligand may stretch or compress the M−N bond lengths in response to this size mismatch. As an example, the ligand strain energy of a hexadentate-coordinated $[ML^6]^{n+}$ complex in the present crystallographically observed *trans-eq,-eq* conformation is shown in Figure 3 for comparison.

The self-exchange electron transfer rate constants given in Table 3 show some interesting features, particularly the 2 orders-of-magnitude variation in k_{11} between the pairs of *trans* and *cis* isomeric hexaamines $[CoL^1]^{3+/2+}$/$[CoL^2]^{3+/2+}$ and $[CoL^3]^{3+/2+}$/$[CoL^4]^{3+/2+}$. The $[CoL^6]^{3+/2+}$ system (bearing a *trans* diamino-substituted macrocycle) shows a k_{11} similar value to that of the other *trans* hexaamines $[CoL^1]^{3+/2+}$ and $[CoL^3]^{3+/2+}$. We have already noted that there are significant differences between the coordination geometries of *trans* and *cis* diamino-substituted tetraaza macrocycles, particularly with respect to their Co−N bond lengths. Molecular mechanics calculations have revealed that intraligand strain in hexadentate coordinated complexes of the *trans* hexaamines L^1 and L^3 leads to "compressed" coordination geometries,[23] due to a mismatch between metal ion size and the preferred cavity sizes of the hexadentate coordinated macrocycles. These calculations have been verified by the X-ray crystal structures of several hexadentate coordinated complexes of L^1 and L^3 which all exhibit remarkably short M−N bond lengths by comparison with other hexaamines.[6,9] By comparison, molecular mechanics calculations have correctly predicted that the *cis* isomeric analogues will lead to "normal" coordination geometries, with M−N bond lengths similar to those found in analogues such as $[M(en)_3]^{n+}$ and $[M(NH_3)_6]^{n+}$. That is, intraligand strain plays a vital role in the observed ground state geometries of complexes of L^{1-4}. We will now consider whether it is an important factor in explaining the observed variations in self-exchange rate constants.

This model is a variation on the entatic state hypothesis of electron transfer reactions,[3,26,27] where a lowering of the classical barrier height of the reaction is achieved through a ligand effected distortion which brings one or both of the reactants closer to the transition state. We have examined the contribution of strain energy to the self-exchange electron transfer reactions of each (hexaamine)cobalt(III/II) system shown in Table 3. The overall strain energy has been plotted as a function of the Co−N bond length *i.e.* along the totally symmetric CoN_6 vibrational coordinate, since this is the most significant structural variable during the reaction. That is, the transition state is reached by a concurrent lengthening of the Co^{III}−N bond lengths and compression of the Co^{II}−N bonds. As an example, the $[CoL^6]^{3+/2+}$ system is shown in Figure 4, with the remaining data appearing in the Supporting Information. In this case, distortions of the Co−N bond lengths do contribute to the overall strain energy in contrast to the plots in Figure 3 where the energies are metal ion independent. The resulting potential energy curves in Figure 4 (for a pair of reactants in the same conformation) intersect where their geometries and strain energies are identical. That is, the intersection describes the transition state of the self-exchange electron transfer reaction in terms of the molecular mechanics model. Note that, in Figure 4, a conformational change from the *trans-eq,ax* to the *trans-eq,eq* conformer occurs in the Co^{II} complex before the transition state is reached, and electron transfer is predicted to occur in the crystallographically observed conformation, although this should not be the ground-state conformation of the Co^{II} complex. The sum of the energy *differences* between the two ground-state geometries and the intersection of the curves (depicted by the two arrows in Figure 4) leads to the strain energy contribution (ΔU_{tot}) to the overall activation free energy for the self-exchange electron transfer reaction ($\Delta G_{exch}^{\ddagger}$). The remaining strain energy changes are given in Table 3.

A change in the overall activation free energy ($\Delta G_{exch}^{\ddagger}$) of ~5.7 kJ mol^{-1} corresponds to a 1 order-of-magnitude variation

(26) Valee, B. L.; Williams, R. J. P. *Proc. Nat. Acad. Sci.* **1968**, *59*, 498.
(27) Pizer, R. *ACS Symp. Ser.* **1982**, *No. 198*, 127.

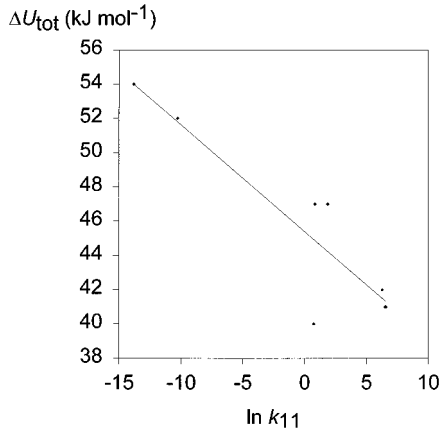

Figure 5. Plot of changes in molecular mechanics strain energy upon activation (ΔU_{tot}) as a function of the observed self-exchange rate constant ln k_{11}.

in the observed self-exchange rate constant at 298 K.[28] We have plotted the strain energy change (ΔU_{tot}) as calculated above *vs* ln k_{11} (Figure 5). The data show a fair correlation ($r^2 = 0.8$), but the slope of the line of best fit is -0.6 kJ mol^{-1} rather than $-RT$ (-2.5 kJ mol^{-1}), which indicates that other factors also contribute to the variations in self-exchange rate constant. The strain energy *changes* from system to system underestimate the observed changes in $\Delta G_{exch}^{\ddagger}$, so there are other variables which remain unaccounted in the present analysis. It has been noted[29] that Franck−Condon and Coulombic work terms are the major contributors to the overall $\Delta G_{exch}^{\ddagger}$ values. However, subtle variations in electronic factors or differences in the outer-sphere reorganizational energy terms can effect changes of several orders-of magnitude in the overall rate constant. Interestingly, a fair correlation between $-\log k_{11}$ and the number of amine H atoms has been noted[1] which suggests significant differences in outer-sphere contributions across the series of (hexaamine)cobalt(III/II) complexes, including variations in ion size and hydrophilicity of the reactants. There does not appear to be an all-encompassing explanation for the remarkable variation in $Co^{III/II}$ hexaamine self-exchange rate constants, but changes in intramolecular strain energy are well correlated as shown in Figure 5.

A final point of interest concerns the particularly high energy d−d electronic maxima that were obtained from the solution electronic spectrum of $[CoL^6]^{3+}$. The crystal structure conformations of $[CoL^6]^{3+}$ and the closely related $[CoL^1]^{3+}$ are the same, and the Co−N bond lengths in the latter complex (Co−$N_{sec,prim}$ 1.937(2), 1.945(2) Å) are comparable with those found in the present structure (Co−$N_{sec,prim}$ 1.946(3), 1.942(3) Å). However, the significantly higher energy electronic maxima of $[CoL^6]^{3+}$ compared with $[CoL^1]^{3+}$ cannot be explained simply by reference to their crystal structure geometries alone. It has been established that hexadentate coordinated complexes of L^1 and L^3 may exhibit a number of conformations,[23] and solution NMR spectroscopy has shown that the complex $[CoL^1]^{3+}$ actually exists in solution as a 1:1 mixture of the *trans-eq,eq* (*trans-ax,eq* + *trans-eq,ax*) conformers.[9] Molecular mechanics and angular overlap model calculations have indicated[30] that the two conformations *trans-eq,eq* and *trans-ax,eq* (referred to as *trans-*$\lambda\delta$ and *trans-*$\delta\delta$ in the reference) will exhibit significantly different electronic maxima, with the former possessing shorter Co−N bond lengths and hence higher energy maxima. Therefore, mixtures of these conformers will yield electronic maxima that are weighted averages of the two pure conformations. In the case of $[CoL^6]^{3+}$, molecular mechanics calculations indicate that the crystallographically observed *trans-eq,eq* conformation is 10 kJ mol^{-1} more stable than any other conformer and, thus, will be dominant in solution at room temperature. Therefore, the higher energy solution electronic maxima of $[CoL^6]^{3+}$ compared with $[CoL^1]^{3+}$ is a consequence of mixing in significant proportions of conformations (*i.e. trans-eq,ax/trans-ax,eq*) with lower energy electronic maxima in the latter case, whereas the $[CoL^6]^{3+}$ exists in one conformation.

Conclusions

Previous work has demonstrated that the geometric disposition of the pendent primary amines in the Co^{III} complexes of L^{1-4} has a marked effect on the structural and spectroscopic properties of the complex. The new complex $[CoL^6]^{3+}$ also behaves similarly when compared with the *trans* diamino-substituted analogues $[CoL^1]^{3+}$ and $[CoL^3]^{3+}$, exhibiting short Co−N bond lengths, a particularly negative $Co^{III/II}$ redox couple, and high-energy d−d electronic maxima. We have shown that $Co^{III/II}$ hexaamine self-exchange rate constant variations of *ca.* 9 orders of magnitude can be modeled in a semiquantitative way by relatively simple molecular mechanics calculations. The conclusion is that changes in strain energy during the electron transfer process account for a considerable amount of the overall activation free energy for self-exchange electron transfer reactions of $Co^{III/II}$ hexaamine systems.

Acknowledgment. We gratefully acknowledge financial support from the University of Queensland, the Australian Institute of Nuclear Science and Engineering, and the Energy Research and Development Corp.

Supporting Information Available: Tables of full crystal data, atomic coordinates, bond lengths and angles, and thermal parameters, plots of strain energy as a function of Co−N bond lengths for the systems $[Co(NH_3)_6]^{3+/2+}$, $[Co(en)_3]^{3+/2+}$, $[CoL^1]^{3+/2+}$, $[CoL^2]^{3+/2+}$, and $[CoL^7]^{3+/2+}$, and plots of k_{obs} *vs* $[Co^{III}]$ for all Zn^+ cross reactions (26 pages). Ordering information is given on any current masthead page.

IC961345E

(28) $\Delta G_{exch}^{\ddagger} = -RT \ln k_{11} - RT \ln Z$; we have assumed no variation in Z across this series.

(29) Endicott, J. F.; Kumar, K.; Ramasami, T.; Rotzinger, F. P. *Prog. Inorg. Chem.* **1983**, *30*, 141.

(30) Bernhardt, P. V.; Comba, P. *Inorg. Chem.* **1993**, *32*, 2798.